Temperature variation in liquid infiltration and defiltration in a MCM41

Aijie Han,[1] Weiyi Lu,[1] Venkata K. Punyamurtula,[1] Taewan Kim,[2] and Yu Qiao[1,2,a)]
[1]*Department of Structural Engineering, University of California-San Diego, La Jolla, California 92093, USA*
[2]*Program of Materials Science and Engineering, University of California-San Diego, La Jolla, California 92093, USA*

(Received 17 April 2008; accepted 6 December 2008; published online 23 January 2009)

In a calometric measurement of infiltration and defiltration of pressurized liquid in a hydrophobic MCM41, it is observed that in nanopores the energy change between solid and liquid phases is dependent on the direction of liquid motion: liquid infiltration is exothermic and liquid defiltration is endothermic. The sorption curves and the temperature variation are insensitive to the loading rate. The magnitude of temperature decrease in defiltration is smaller than the temperature increase in infiltration, fitting well with the hysteresis of the sorption curve. These phenomena can be attributed to the confinement effect of nanopore walls and the thermally/mechanically aided surface diffusion of liquid molecules. © *2009 American Institute of Physics*. [DOI: 10.1063/1.3068328]

I. INTRODUCTION

Understanding nanofluidic behaviors has been increasingly important to the studies on materials processing, molecular transport, chemical sensing, etc.[1–4] Over the years, a large number of computer simulations have been carried out to explore the details of liquid-solid interaction in nanoenvironment.[5–7] For instance, it was predicted that water molecules can rapidly transport across a short carbon nanotube, forming a chainlike structure.[8,9] If the nanochannel size is relatively large, the structure of confined liquid molecules may exhibit layered characteristics, depending on the liquid and solid species as well as the boundary condition.[10–12] In these studies, it was assumed that the temperature is constant and the temperature field is always in equilibrium, i.e., the environment could be regarded as an infinitely large heat reservoir.[13] The liquid conduction was often reversible, which was compatible with the experimental data that, as water molecules moved across an array of carbon nanotubes, the effective viscosity was much smaller than that of the bulk phase.[14,15]

In a recent experiment on nanoporous silica, it was confirmed that as the nanopore surfaces were hydrophobic, a sufficiently high external pressure must be applied to overcome the capillary effect; otherwise liquid infiltration could not occur.[16,17] Unlike the prediction of computer simulations for carbon nanotubes, the liquid motion in silica nanopores was irreversible. When the external pressure was lowered, liquid defiltration was much more difficult than liquid infiltration, causing a significant hysteresis of the sorption curve. To understand the fundamental mechanisms, it becomes imperative to answer the following question: what is the mechanism of energy exchange of confined liquid?

In a large channel, the flow of a viscous liquid is exothermic.[15] Usually, no-slip assumption can well describe the solid-liquid boundary condition. Inside the boundary layer, liquid molecules are adsorbed by solid surface; in the interior, a parabolic velocity profile would be developed, as a pressure difference exists along the flow direction.[16] The shear stress among liquid molecules leads to heat generation. Thus, the system entropy increases. In a nanoenvironment, the continuum theory breaks down. Across the cross section of a nanopore the number of liquid molecules is limited, and thus the velocity profile can be quite random.[18] The motion of liquid molecules along the nanotube/nanochannel surface may be frictionless, since no energy dissipation would be directly involved in the liquid-solid interaction.[19,20] Under this "ideal" condition, liquid infiltration and defiltration should be an isothermal process.[21] However, currently, experimental data of energy exchange of nanofluidics are rare.[22]

II. EXPERIMENTAL

In the current research, we investigated a MCM41. The network material was obtained from Aldrich, with the modal value of nanopore size of 1.9 nm and the specific nanopore surface area of 1060 m^2/g. The material characterization was performed by using a TriStar-3000 gas absorption analyzer. The as-received material was in powder form, with the particle size in the range of 10–50 μm. Following vacuum drying at 100 °C for 4 h, the MCM41 was mixed with 40 ml of dry toluene and 0.5 ml of chlorotrimethylsilane at 90 °C for 4 h. The mixing rate was about 20 rpm. During this process, negatively charged hydroxyl sites were replaced by $(CH_3)_3SiO$ groups, and thus the material became hydrophobic.[23] The surface treated material was thoroughly rinsed by dry toluene and warm water, and vacuum dried at 80 °C for 12 h.

The pressure induced infiltration (PII) experiment was carried out in a Type 5580 Instron machine. As shown in Fig. 1, in a bilayer cylinder, a mixture of 1 g of surface treated MCM41 and 5 g of saturated sodium chloride solution was sealed by a piston. Sodium chloride was used to promote liquid "outflow,"[24] so that both infiltration and defiltration

a)Author to whom correspondence should be addressed. Electronic mail: yqiao@ucsd.edu.

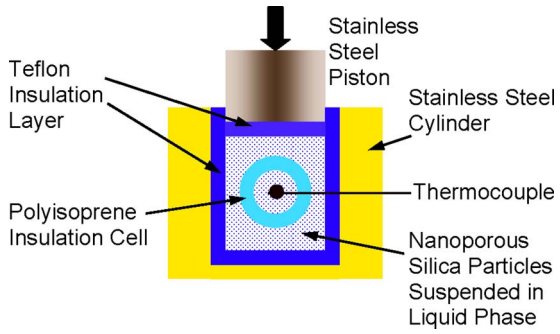

FIG. 1. (Color online) Schematic of the calometric measurement system.

could be investigated. The supporting (outer) layer was made of stainless steel and the insulation (inner) layer was made of Teflon. The piston was also insulated by a layer of Teflon. A type *E* thermocouple was placed inside the cylinder to measure the temperature change in the liquid phase. Surrounding the thermocouple, an additional polyisoprene (PI) insulation cell was employed to further prevent heat loss. The solid/liquid ratios inside and outside the PI cell were the same.

The liquid phase was driven into the nanopores by a quasihydrostatic pressure. The pressure was applied by compressing the piston into the cylinder. The loading rate, which was in the range of 0.1 to 10 mm/min, was constant in the PII test. The piston was moved back when the pressure reached 50 MPa. Once the pressure was reduced to zero, the loading-unloading process was repeated for a few times. Figure 2 shows typical sorption curves, and Fig. 3 shows typical temperature measurement results. Since in all the loading cycles following the first one, the sorption curves and the temperature profiles were quite similar, the following discussion will be focused on the first two loadings.

III. RESULTS AND DISCUSSION

From Fig. 2, it can be seen that if the pressure is lower than 18 MPa, the liquid phase cannot enter the nanopores in MCM41, and thus the system compressibility is quite small. As the pressure exceeds 18 MPa, an infiltration plateau ("AB") is formed, indicating that PII takes place. As the nanopores are filled, the infiltration plateau ends and the system becomes nearly incompressible again ("BC"). Upon unloading, the confined liquid does not defiltrate until the pressure is much lower than the infiltration pressure, and thus the

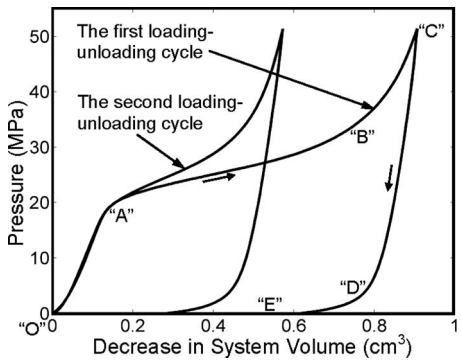

FIG. 2. Typical sorption curves. The curves have been shifted along the horizontal axis.

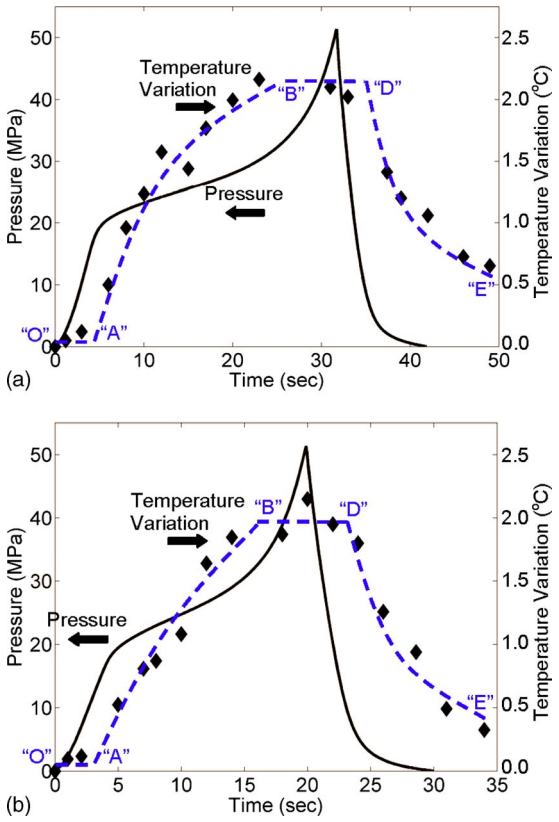

FIG. 3. (Color online) Temperature variation during the infiltration-defiltration process: (a) the first loading-unloading cycle and (2) the second loading-unloading cycle. The solid lines and the diamond symbols indicate the testing data of pressure and temperature variation, respectively; and the dashed lines are schematic curves of temperature variation.

slope of Section "CD" is close to that of Section "BC." When the pressure is lower than 5 MPa, defiltration begins, accompanied by the formation of a defiltration plateau ("DE"). At the second loading, the sorption curve is similar to that of the first loading, except that the width of infiltration plateau is smaller, suggesting that the defiltration in the first cycle is incomplete. That is, only a part of confined liquid comes out; the rest of nanoporous space remains being filled, and thus are not involved in the infiltration process in following loading cycles. As the loading cycle is repeated, no further variation in sorption curve can be detected. The partial "nonoutflow" may be related to the nonuniform distribution of surface groups, especially in the interior of nanopores.

As the loading rate changes from 0.1 to 10 mm/min by 100 times, the measured sorption curves are nearly the same, which clearly shows that liquid motion in nanopores cannot be described by continuum theory. According to the classic Poiseuille solution,[25] in a viscous flow the pressure gradient should be proportional to the flow rate. In a nanopore, since there are only a small number of liquid molecules in the cross section, as demonstrated in computer simulations,[8,9,13] liquid molecules may slide against solid surface. Since the velocity difference among the liquid molecules is not as regular as that in a continuum flow, also because that the characteristic velocity of continuum flow is much smaller than that of thermal vibration of molecules, the rate depen-

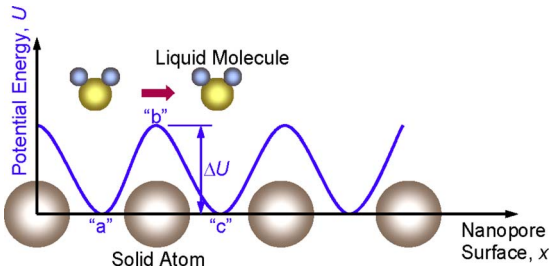

FIG. 4. (Color online) Schematic of a confined liquid molecule in a nanopore.

dence of pressure gradient is negligible. Without the viscosity effect, other factors that dominate the interactions of liquid and solid molecules, such as the Van der Waals force and the Coulomb force, are intrinsically nondissipative; i.e., the motion of the liquid molecule may be "frictionless," which is in agreement with the fact that a liquid phase does not carry shear loadings. Under this condition, no temperature change should be expected during liquid infiltration or defiltration.

The experimental data of temperature variation (Fig. 3), however, show that the above analysis is invalid. On the one hand, associated with infiltration, a considerable temperature increase, "AB," is measured, which is somewhat similar with the prediction of continuum theory of viscous flow. On the other hand, during defiltration, the temperature decreases ("DE"), which is contradictory to the continuum theory. Note that while it has been while known that water adsorption process can be exothermic and water desorption can be endothermic, it does not explain the fact the amount of temperature increase associated with infiltration is larger than the amount of temperature decrease associated with defiltration. Before the onset of infiltration ("OA") and between infiltration and defiltration ("BD"), the temperature change is negligible, indicating that compression of liquid phase is an elastic process, as it should be.

The temperature variation may be attributed to the confinement of nanopore walls. In a nanopore, the motion of a liquid molecule along the radius direction can be significantly suppressed, especially when the nanopore surface is nonwettable. That is, as a liquid molecule move along the axial direction of a nanopore, it has to overcome the energy barrier between tetrahedral sites, as shown in Fig. 4. From a low-potential location ("a") to a high-potential location ("b"), the molecular velocity tends to decrease, and from "b" to "c" it tends to increase. Note that in the experiment the infiltration rate is determined by the piston speed, which is constant. Thus, from "a" to "b," additional work must be done by the external loading, so that the system free energy increases and the molecule velocity remains constant. From "b" to "c," because the nanopore wall is of a finite heat conductivity, the excess kinetic energy of the liquid molecule would be absorbed by atoms in the solid phase; thus, the infiltration process is exothermic. The dissipated energy causes an effective "internal friction." During defiltration, a confined liquid molecule must absorb thermal energy from the environment to overcome the energy barrier between "c" and "a," and therefore the process becomes endothermic. That is, the temperature variation associated with the liquid motion in nanopore is caused by the mechanically/thermally aided surface diffusion, independent of the liquid viscosity, which explains why the sorption curves are rate insensitive. This analysis agrees well with a previous experimental observation that, as temperature increases, the infiltration pressure tends to decrease while the defiltration volume can be largely increased, since at a higher temperature the mobility of liquid molecules is larger and consequently both liquid infiltration and defiltration become easier.

Through a differential scanning calorimetry test, the heat capacity of the silica-liquid mixture was determined as $\xi = 3.5$ J/g K. During infiltration, the temperature increase is $\Delta T_1 = 2.2$ °C, and the associated energy exchange is $U_e = m\xi\Delta T = 46$ J, or 4×10^{-14} μJ/nm^2 over the entire nanopore surface, where $m = 6$ g is the total mass of the mixture of nanoporous silica and liquid. According to potential functions commonly used in molecular dynamics simulations,[26] the energy barrier ΔU should be about 10 kJ/mol or around 10^{-14} μJ per atom. If in each nm^2 of nanopore surface there is one surface group, the total energy that liquid molecules must overcome to move across solid surface is around 10^{-14} μJ/nm^2, at the same level as the heat generation measured in the experiment.

During defiltration, the temperature decreases by about 1.6 °C, which corresponds to an energy exchange of 3×10^{-14} μJ/nm^2. That is, to diffuse out of the nanopore, the thermal energy absorbed by a liquid molecule is nearly 3/4 of the dissipated energy during infiltration, even though the infiltration rate and the defiltration rate are nominally the same. The difference between them may be related to the inefficient thermal conduction in silica phase, the reduction in liquid molecule pileup in defiltration, and the "ink bottle" effect of irregular nanopore walls that lowers the defiltration energy barrier, the details of which are still under investigation. Note that the above calculations provide only an order-of-magnitude assessment of energy exchanges involved in the liquid infiltration and defiltration process. A more accurate estimate should be given by computer simulation.

Since the temperature increase in infiltration is larger than the temperature decrease in defiltration, after the first loading-unloading cycle the system temperature increases by 0.6 °C. According to the sorption curve shown in Fig. 2, the dissipated energy can be estimated as the area enclosed by the hysteretic loading-unloading path, about 18 J. It should cause a temperature increase of 0.8 °C, which is comparable with but larger than the result of energy exchange analysis, probably because that a part of the mechanical work is converted to the excess solid-liquid infiltration tension of confined liquid that does not defiltrate after the external pressure is fully removed.

At the second loading, through Fig. 3(b), it can be seen that the characteristics of temperature variation are similar with that at the first loading: liquid infiltration is exothermic and liquid defiltration is endothermic, suggesting that the partial nonoutflow is not a key factor affecting the temperature variation. The temperature increase is smaller, since the nanopores occupied by the non-outflow liquid are not involved in the energy exchange. The net temperature increase after the defiltration completes is only 0.4 °C, much smaller

than that in Fig. 3(a). According to Fig. 2, the net dissipated energy in the second loading cycle is nearly 11 J, which should cause a temperature change of 0.5 °C, close to the measurement result.

Note that in both the first and the second loading cycles, the temperature increase in infiltration and the temperature decrease in defiltration are nonlinear. The temperature variation is more pronounced at the beginning stage of infiltration/defiltration, which may be associated with the nanopore size distribution. With the aid of an external pressure, guest species tend to be active in smaller nanopores,[27] where the specific surface area is larger. Thus, at the onset of infiltration/defiltration, the energy density is higher, leading to the rapid temperature variation. As the infiltration/defiltration continues, more nanopores are involved and the average rate of thermal energy generation or absorption is reduced.[28]

IV. CONCLUDING REMARKS

In summary, the current study is focused on calometric experiment of liquid motion in nanopores of a MCM41. The liquid infiltration is exothermic, i.e., there exists an effective internal friction. The liquid defiltration is endothermic. The sorption curves and temperature profiles are independent of the loading rate. The temperature increases more profoundly in infiltration than it decreases in defiltration, leading to a net temperature change after a complete loading-unloading cycle, which fits with the overall energy dissipation measurement. These unique phenomena can be related to the confinement effect of nanopore walls and the surface diffusion of confined liquid molecules that is thermally and/or mechanically aided.

ACKNOWLEDGMENTS

The experiment was supported by The Army Research Office under Grant No. W911NF-05-1-0288. The analysis was supported by The National Science Foundation under Grant No. CMS-0623973. Special thanks are also due to Professor Vistasp M. Karbhair for the help with the differential scanning calorimetry measurement.

[1] P. Kohli, C. C. Harrell, Z. H. Cao, R. Gasparac, W. H. Tan, and C. R. Martin, Science **305**, 984 (2004).
[2] A. A. Gusev and O. Guseva, Adv. Mater. (Weinheim, Ger.) **19**, 2672 (2007).
[3] D. A. Dikin, S. Stankovich, E. J. Zimney, R. D. Piner, G. H. B. Dommett, G. Evmenenko, S. T. Nguyen, and R. S. Ruoff, Nature (London) **448**, 457 (2007).
[4] L. Sun, F. Banhart, A. V. Krasheninnikov, J. A. Rodriguez-Manzo, M. Terrones, and P. M. Ajayan, Science **312**, 1199 (2006).
[5] G. Q. Hu and D. Q. Li, Chem. Eng. Sci. **62**, 3443 (2007).
[6] D. Mijatovic, J. C. T. Eijkel, and A. van den Berg, Lab Chip **5**, 492 (2005).
[7] A. Holtzel, U. Tallarek, and J. Separ, Science **30**, 1398 (2007).
[8] G. Hummer, J. G. Rasalah, and J. P. Noworyta, Nature (London) **414**, 188 (2001).
[9] C. Dellago and G. Hummer, Phys. Rev. Lett. **97**, 245901 (2006).
[10] P. D. Ashby and C. M. Lieber, J. Am. Chem. Soc. **126**, 16973 (2004).
[11] D. Takaiwa, K. Koga, and H. Tanaka, Mol. Simul. **33**, 127 (2007).
[12] M. Rossi, D. E. Galli, and L. Reatto, Phys. Rev. B **72**, 064516 (2005).
[13] Y. Qiao, G. Cao, and X. Chen, J. Am. Chem. Soc. **129**, 2355 (2007).
[14] M. Majumder, N. Chopra, R. Andrews, and B. J. Hinds, Nature (London) **438**, 44 (2005).
[15] J. K. Holt, H. G. Park, Y. M. Wang, M. Stadermann, A. B. Artyukhin, C. P. Grigoropoulos, A. Noy, and O. Bakajin, Science **312**, 1034 (2006).
[16] A. Han and Y. Qiao, Chem. Lett. **36**, 882 (2007).
[17] A. Han and Y. Qiao, Langmuir **23**, 11396 (2007).
[18] L. M. Robert, *Applied Fluid Mechanics* (Prentice-Hall, Englewood Cliffs, 2006).
[19] T. Z. Qian, X. P. Wang, and P. Sheng, Comm. Comp. Phys. **1**, 1 (2006).
[20] P. Koumoutsakos, Annu. Rev. Fluid Mech. **37**, 457 (2005).
[21] C. Neto, D. R. Evans, E. Bonaccurso, H. J. Butt, and V. S. J. Craig, Rep. Prog. Phys. **68**, 2859 (2005).
[22] J. S. Ellis and M. Thompson, Phys. Chem. Chem. Phys. **6**, 4928 (2004).
[23] M. H. Lim and A. Stein, Chem. Mater. **11**, 3285 (1999).
[24] X. Kong and Y. Qiao, Appl. Phys. Lett. **86**, 151919 (2005).
[25] C. T. Crowe, D. F. Elger, and J. A. Roberson, *Engineering Fluid Mechanics* (Wiley, New York, 2006).
[26] M. P. Allen and D. J. Tildesley, *Computer Simulation of Liquids* (Clarendon, Oxford, 1990).
[27] R. L. Grob and E. F. Barry, *Modern Practice of Gas Chromatography* (Wiley-Interscience, New York, 2004).
[28] X. Kong and Y. Qiao, Philos. Mag. Lett. **85**, 331 (2005).